Insertion of a Coiled-Coil Peptide from Influenza Virus Hemagglutinin into Membranes

Yeon Gyu Yu, David S. King, Yeon-Kyun Shin*

The trimeric protein hemagglutinin (HA) of the influenza viral envelope is essential for cell entry. To investigate the interaction of HA with membranes, two 40-residue, cysteine-substituted peptides comprising the loop region and the first part of the coiled-coil stem were synthesized and modified with a nitroxide spin label. Electron paramagnetic resonance analysis revealed that the peptide inserts reversibly into phospholipid vesicles under endosomal pH conditions. This result suggests that some or all of the long coiled-coil trimer of HA may insert into membranes, which could bring the viral and cell membranes closer together and facilitate fusion.

Influenza virus enters the cell through endocytosis and crosses into the cytoplasm by fusion with endosomal membranes. In the endosome, low pH (~5.5) triggers a conformational change in HA to a fusogenic form that then brings about fusion of the two membranes. HA is a homotrimer in which each subunit consists of a sialic acid–binding domain (HA1) and a "fusion peptide"–containing domain (HA2). In the native state, the HA2 domain contains a helical hairpin structure, a short helix that is connected by means of a 28-residue loop to a long helical stem protruding from the viral membrane (*1*) (Fig. 1A). However, this loop region has been found to have a high coiled-coil propensity (*2*). According to predictions from the study of model peptides, this loop region may undergo a loop-to-helix conformational change after dissociation of HA1 head domains (*3*) under endosomal low pH, resulting in the extension of the coiled-coil stem of the native state.

We studied by electron paramagnetic resonance (EPR) the membrane binding properties of a 40-residue region (L40) of HA, comprising the long loop and the first part of the long α-helical stem of HA2. Two cysteine substitution mutants, L40H64C and L40V84C (Fig. 1B), were synthesized and labeled with a sulfhydryl-specific methanethiosulfonate nitroxide spin label **1** (*4*). The solution properties of a 36-residue peptide from this area have been well characterized by Carr and Kim (*2*), who showed that this sequence reversibly forms a three-stranded coiled coil in acidic conditions. Moreover, 11 of its 40 residues are acidic, making it a likely candidate for the acid-sensitive switch for trimerization and membrane interaction.

The relatively narrow three-line EPR spectrum at pH 6.9 indicates that the peptide is predominantly in the monomeric random-coil state (Fig. 2). On the other hand, at low pH an equilibrium between the random-coil species and the trimeric coiled coil is expected (*2*). In the expected parallel registered coiled coil, motion of the attached nitroxide would be much retarded because of secondary structure formation and the increase of hydrodynamic radius. Moreover, fairly strong spin-spin interactions are expected because the nitroxides are close to each other. Thus, the EPR spectral lines from the trimer should be substantially broadened. The solution spectra at low pH display mainly the spectral component from the random-coil species with reduced intensity, plus a broad spectral component from the trimer species identified in the integrated spectrum (Fig. 2). Upon increase of the pH to neutrality, the full EPR intensity is recovered. These spectral changes are consistent with an equilibrium of the random coil and the registered trimer. The calculated equilibrium constants at various pH values were nearly identical for both spin-labeled mutants (*5*).

On the other hand, the EPR spectrum of L40H64C in the presence of vesicles at pH 5.2 (Fig. 3A) is similar to the spectra of other spin-labeled peptides such as melittin (*6*) and alamethicin (*7*) when they become bound to membranes. The estimated rotational correlation time, τ_R, is approximately 3 ns, which is typical for nitroxides on membrane-bound peptides (*8*). Moreover, we do not observe the narrow spectral component arising at higher pH (Fig. 3, B and C), suggesting that all of the peptide is inserted into the membrane. Several other features of the EPR spectra indicate that the nitroxide faces the hydrophobic hydrocarbon chains of the bilayer in the membrane-inserted state. First, the solvent-sensitive hyperfine splitting corresponds to a relatively nonpolar environment and is similar to that for the same nitroxide on the external surface of proteins embedded in membranes (*9*). Second, the nitroxide is inaccessible to collision with chromium oxalate, which partitions dominantly into the water phase, whereas the collision rate with nonpolar oxygen, which partitions preferentially into the lipid phase, is very high.

For L40V84C, the change in line shape upon membrane insertion is similar to that of L40H64C (Fig. 3D). The reduced hyperfine coupling constant and the strong collision rate with oxygen are also consistent with the nitroxide being in the bilayer. However, we observed some collision with chromium oxalate, indicating that the ni-

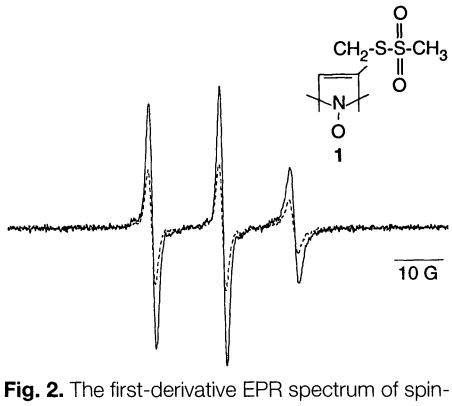

Fig. 2. The first-derivative EPR spectrum of spin-labeled L40H64C at pH 6.9 and 20°C (solid line) superimposed on that at pH 5.1 (dotted line). The peptide concentration was 8 μM in buffer A (100 mM NaCl, 50 mM citric acid, and 50 mM sodium phosphate adjusted to the indicated pH with 2 M NaOH). In the inset figure, **1** represents the nitroxide spin label **1**.

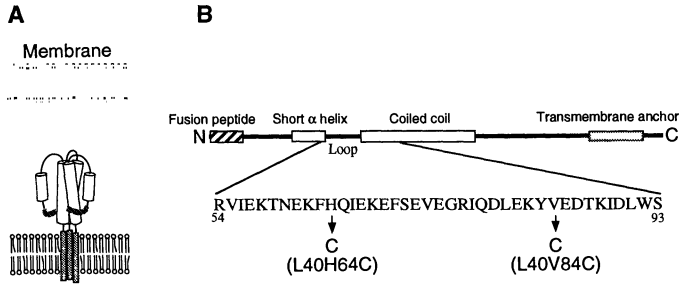

Fig. 1. (**A**) The native state of HA2. Cylinders, stippled regions, and hatched regions represent α helices, COOH-terminal transmembrane domains, and fusion peptides, respectively. (**B**) Diagram of the structural elements of the HA2 domain; the amino acid sequence of the selected peptide region and the cysteine-substituted positions are indicated underneath. Single-letter abbreviations for the amino acids are as follows: C, Cys; D, Asp; E, Glu; F, Phe; G, Gly; H, His; I, Ile; K, Lys; L, Leu; N, Asn; Q, Gln; R, Arg; S, Ser; T, Thr; V, Val; W, Trp; and Y, Tyr.

Y. G. Yu and Y.-K. Shin, Department of Chemistry, University of California, and Structural Biology Division, Lawrence Berkeley Laboratory, Berkeley, CA 94720, USA.
D. S. King, Howard Hughes Medical Institute and Department of Molecular and Cell Biology, University of California, Berkeley, CA 94720, USA.

*To whom correspondence should be addressed.

troxide in this case is likely in the phospholipid head group region. The results of this EPR analysis of the spin-labeled variants L40H64C and L40V84C at 20°C strongly support the idea that both the NH_2- and COOH-terminal regions of the peptide are in the bilayer, although their exact orientation there is unclear.

At low temperatures, the trimer has been found to be much stabilized (*2*). Consistent with this observation, the amplitude of the solution spectrum of L40H64C at 2°C is very small (Fig. 3E): Approximately 95% of the peptide is trimeric at a total peptide concentration of 10 μM. On the other hand, the spectra in vesicles are similar to those at higher temperature (Fig. 3A) but show reduced motion. These characteristics indicate that the peptide inserts into the bilayer at 2°C despite significant stabilization of the trimer.

According to our EPR data, both peptides in a membrane are likely monomeric. We do not observe any spectral features arising from spin-spin interactions. In addition, the relatively fast τ_R and strong collision rates with oxygen for both spin-labeled variants indicate that the nitroxides are free of interactions with other peptides, similar to the situation with spin-labeled melittin in membranes (*6*).

Adhesion of the fusion peptide to the target membrane after the conformational change triggered by low pH is a rapid and irreversible step (*10*). Photoaffinity labeling of HA2 to phospholipids derived from cyanobenzoic acid has been observed and increases after the onset of membrane fusion (*10*, *11*). Labeling of HA2 during fusion may be partly a consequence of membrane insertion of the coiled coil.

To investigate the relevance of membrane insertion of the peptide to HA-induced membrane fusion that occurs under endosomal low pH conditions, we examined the pH dependence of peptide insertion into membranes. After increasing pH, we observed an increase of the narrow spectral component (Fig. 3, B and C), indicating the existence of random-coil species in the water phase. The pH dependence of membrane insertion of L40H64C correlates well with that of HA-induced membrane fusion (Fig. 4). The transition midpoint of L40V84C is ~0.2 pH units lower.

Obviously, the protonation of acidic residues is required for membrane insertion. The insertion of such a hydrophilic peptide into membranes is unusual, although it does not seem completely unreasonable after the multiple negative charges are mitigated at low pH. Approximately 80% of spin-labeled L40H64C inserts into neutral vesicles of 1-palmitoyl-2-oleoyl phosphatidylcholine at pH 5.0. Because the pH dependence is similar to that of insertion into negatively charged membranes, the driving force for membrane insertion is probably hydrophobic (*12*).

We propose the following model (Fig. 5). Insertion of the coiled-coil region into the membrane would be preceded by the conformational change that untethers the hairpin structure of HA2 (*3*, *13*). After the initial adhesion of the fusion peptide to the target membrane, we envision rapid insertion of the coiled coil into the membrane at even higher pH than that for the soluble peptide because the membrane surface pH would be lower than the bulk pH and there could be effects of the reduced dimensionality (*14*). We also speculate that once the coiled-coil trimer gets embedded in the membrane, the hydrophobic helix interfaces become solvated by hydrocarbon chains of phospholipids and the trimer comes apart (Fig. 5).

Proceeding to the formation of the hemifusion intermediate and the fusion pore (*15*) after insertion of the fusion peptide into the target membrane, we propose that membrane insertion of the coiled-coil domain helps bring about juxtaposition of the two membranes. Cooperative interactions of several HA coiled-coil trimers are likely required to overcome the strong repulsive forces operative as two hydrated membranes are brought together (*16*).

Fusion induced by HA can be triggered thermally (above 63°C) at neutral pH (*17*). At high temperature, the α helicity of HA decreases significantly as the HA2 domain becomes denatured (*17*). At physiological temperatures, it is the low pH–induced loop-to-helix transition that is important for fusion (*2*). Thus, the pathways of heat- and pH-induced fusions are probably different. Membrane insertion is not a general property for all amphipathic coiled coils: A well-characterized, 33-residue, coiled-coil peptide from the GCN4 leucine zipper protein (*18*) does not interact with membranes under similar conditions to those in this work.

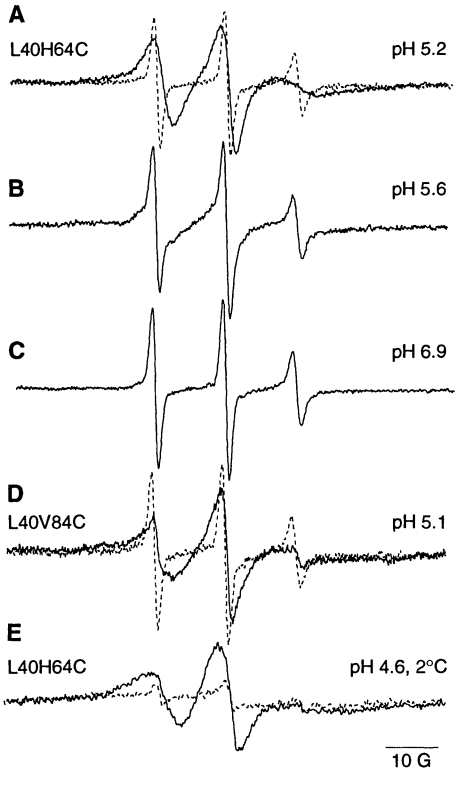

Fig. 3. Changes in EPR spectra of spin-labeled peptides at endosomal pH conditions. (**A** to **C**) L40H64C, 20°C; (**D**) L40V84C, 20°C; (**E**) L40H64C, pH 4.6, 2°C. For (A), (D), and (E), the solid line corresponds to the labeled peptide in the presence of vesicles of 1-palmitoyl-2-oleoyl phosphatidylcholine containing 20 mol% 1-palmitoyl-2-oleoyl phosphatidylglycerol in buffer A (*19*), and the dotted line corresponds to the labeled peptide in the absence of phospholipids. For all samples, the final concentrations of peptides and of phospholipids were 8 to 10 μM and 50 mM, respectively (*20*).

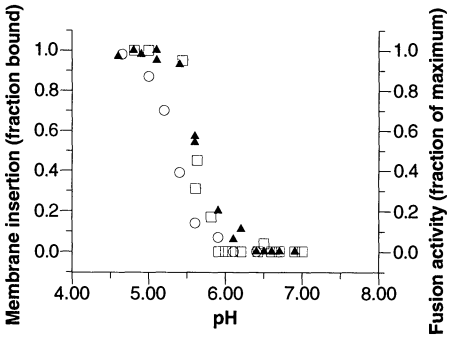

Fig. 4. Membrane-inserted fraction of each peptide and HA-induced membrane fusion as a function of pH (*21*): L40H64C (closed triangles); L40V84C (open circles); HA-induced fusion (open squares) (*22*).

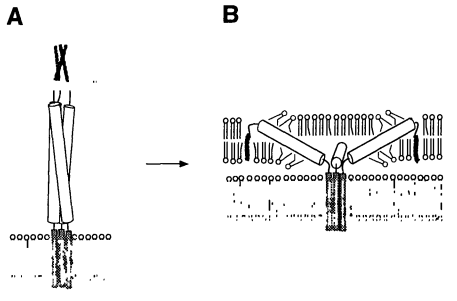

Fig. 5. (**A**) The acid-induced fusogenic state (*2*). (**B**) The proposed fusion intermediate.

REFERENCES AND NOTES

1. I. A. Wilson, J. J. Skehel, D. C. Wiley, *Nature* **289**, 366 (1981).
2. C. M. Carr and P. S. Kim, *Cell* **73**, 823 (1993).
3. R. W. Doms, A. Helenius, J. White, *J. Biol. Chem.* **260**, 2973 (1985); J. M. White and I. A. Wilson, *J. Cell Biol.* **105**, 2887 (1987); A. Puri, F. P. Booy, R. W. Doms, J. M. White, R. Blumenthal, *J. Virol.* **64**, 3824 (1990).
4. The peptides were synthesized with 9-fluorenylme-

thoxycarbonyl (Fmoc) protecting group chemistry and characterized by electrospray-ionization mass spectrometry after reversed-phase high-performance liquid chromatography (HPLC) purification before and after the spin-labeling reaction.
5. Trimerization of the peptide was verified by size-exclusion HPLC at pH 4.8 and 0°C. The thermal unfolding profile monitored by EPR was nearly superimposable on the profile monitored by the circular dichroism signal at 222 nm. The transition midpoint, M_T, was 35°C for both spin-labeled peptides, which is 10°C higher than M_T of the 36-residue peptide in (*2*). This higher thermal stability might be provided by the four additional residues at the COOH-terminus.
6. C. Altenbach and W. L. Hubbell, *Proteins* **3**, 230 (1988).
7. S. J. Archer, J. F. Ellena, D. S. Cafiso, *Biophys. J.* **60**, 389 (1991).
8. The expected τ_R for the trimer with a mass of 15 kD is approximately 7 to 8 ns.
9. The isotropic nitrogen hyperfine coupling constant for the methanethiosulfonate spin label in water, A_N, is 16.4 G. For the same spin label on L40H64C in the membrane-associate state, A_N = 15.1 G, and on residues facing the bilayer interior on the bacteriorhodopsin, A_N = 15.0 G [C. Altenbach, T. Marti, H. G. Khorana, W. L. Hubbell, *Science* **248**, 1088 (1990)].
10. T. Stegmann, J. M. Delfino, F. M. Richards, A. Helenius, *J. Biol. Chem.* **266**, 18404 (1991).
11. M. Tsurudome *et al.*, *ibid.* **267**, 20225 (1992).
12. If a net positive charge is assumed to develop on the peptide at low pH, the increased affinity for negatively charged membranes can be accounted for by the accumulation of the positively charged peptide in the membrane surface layer. Membrane interactions would be enhanced by the Boltzmann factor, $\exp[-\mathbf{z}\Psi]$, where $\mathbf{z}$ is the effective valence of the peptide and Ψ is the surface potential.
13. R. S. Daniels *et al.*, *Cell* **40**, 431 (1985); G. W. Kemble, D. L. Bodian, J. Rose, I. A. Wilson, J. M. White, *J. Virol.* **66**, 4940 (1992).
14. J. Y. Kim *et al.*, *Biophys. J.* **60**, 135 (1991).
15. G. W. Kemble, T. Danieli, J. M. White, *Cell* **76**, 383 (1994); J. M. White, *Science* **258**, 917 (1992).
16. T. Stegmann, R. W. Doms, A. Helenius, *Annu. Rev. Biophys. Biophys. Chem.* **18**, 187 (1989).
17. R. W. Ruigrok *et al.*, *EMBO J.* **5**, 41 (1986).
18. E. K. O'Shea, J. D. Klemm, P. S. Kim, T. Alber, *Science* **254**, 539 (1991).
19. Vesicles extruded through polycarbonate filters with a pore size of 1000 Å were used for all measurements.
20. Below pH 5.0 the EPR spectrum was independent of the peptide-to-lipid ratio above 500, indicating that the membrane-inserted state is not affected by the lipid-to-peptide ratio.
21. The membrane-inserted fraction was approximated by the ratio of the concentration of membrane-inserted species (for example, see the broad component in Fig. 3B) to the total peptide concentration estimated by spectral subtraction analysis.
22. S. A. Wharton, J. J. Skehel, D. C. Wiley, *Virology* **149**, 27 (1986).
23. Supported by the start-up fund from the University of California at Berkeley and by Lawrence Berkeley Laboratory grant 3668-19.

1 April 1994; accepted 15 August 1994

Quantitative Trait Locus for Reading Disability on Chromosome 6

Lon R. Cardon,*† Shelley D. Smith, David W. Fulker, William J. Kimberling, Bruce F. Pennington, John C. DeFries

Interval mapping of data from two independent samples of sib pairs, at least one member of whom was reading disabled, revealed evidence for a quantitative trait locus (QTL) on chromosome 6. Results obtained from analyses of reading performance from 114 sib pairs genotyped for DNA markers localized the QTL to 6p21.3. Analyses of corresponding data from an independent sample of 50 dizygotic twin pairs provided evidence for linkage to the same region. In combination, the replicate samples yielded a χ^2 value of 16.73 (P = 0.0002). Examination of twin and kindred siblings with more extreme deficits in reading performance yielded even stronger evidence for a QTL (χ^2 = 27.35, $P < 0.00001$). The position of the QTL was narrowly defined with a 100:1 confidence interval to a 2-centimorgan region within the human leukocyte antigen complex.

Reading disability (RD), or dyslexia, is a major social, educational, and mental health problem. In spite of average intelligence and adequate educational opportunities, 5 to 10% of schoolchildren have substantial reading deficits (*1*). Clear evidence for familial transmission has existed for almost a century, and results of recent twin and family studies have shown a substantial genetic component to the disorder (*2*), with heritable variation estimated at 50 to 70% (*3*). Mapping QTLs for RD would facilitate identification of the functional genes that cause the disorder and improve risk estimation and early diagnosis.

Several findings indicating possible linkages for RD have been reported. In a study of nine three-generation families selected for a history of specific RD, we previously obtained evidence for a possible linkage on chromosome 15 (*4*). Recently, evidence of linkage has been reported for markers in the Rh region of chromosome 1 (*5*) and with a translocation between 1p and 2q (*6*). Further research with our kindreds has yielded evidence for a linkage on chromosome 6 in the human leukocyte antigen (HLA) region, but not for linkage on chromosome 15 (*5*, *7*). The present report describes results with more informative markers on chromosome 6 in these kindreds and a replication in an independent sample of dizygotic (DZ) twins.

The HLA region was targeted for this study because of a possible association between dyslexia and autoimmune disorders (*8*). Results of previous studies have suggested that rates of autoimmune diseases are elevated in relatives of dyslexic probands and that the incidence of dyslexia is increased in relatives of probands having autoimmune illnesses (*9*). Although the causal basis of the association is unknown, the evidence for association from these independent studies points to the HLA complex as a candidate region.

Our kindred sibling sample comprises 358 individuals from 19 families who were chosen from a variety of sources, including clinics and private schools specializing in RD. Selection criteria included an extended family history of specific RD, as diagnosed by reading performance at least 2 years below expected grade level and in a pattern consistent with autosomal dominant inheritance (*10*). The twin sample comprises 50 families drawn from the Colorado twin study of RD (*3*). The twins range in age from 8 to 20 years (mean, 12.16 years). Twin pairs in which at least one member had a positive school history of reading problems were objectively and systematically selected through cooperating school districts. Individuals were administered a battery of psychometric tests including the Peabody individual achievement tests (PIAT) and the WISC-R intelligence test (*11*). Subjects with verbal or performance IQ of at least 90 were diagnosed on the basis of a composite discriminant score. Discriminant weights for PIAT reading recognition, reading comprehension, and spelling were computed from an independent sample of RD and control nontwin children in order to produce a continuous measure of RD with known psychometric properties. A comparable measure was constructed from the psychometric data obtained on the kindred sample. We refer to this measure as the discriminant score for reading performance.

One advantage of using DZ twins for linkage analysis is that they provide a perfect control for the effects of age. In the kindreds, which span three generations,

L. R. Cardon, Health Sciences Program, SRI International, Menlo Park, CA 94025 and Department of Mathematics, Stanford University, Stanford, CA 94305, USA.
S. D. Smith and W. J. Kimberling, Center for Hereditary Communication Disorders, Boys Town National Research Hospital, Omaha, NE 68131, USA.
D. W. Fulker and J. C. DeFries, Institute for Behavioral Genetics, University of Colorado, Boulder, CO 80309, USA.
B. F. Pennington, Department of Psychology, University of Denver, Denver, CO 80208, USA.

*To whom correspondence should be addressed.
†Present address: Sequana Therapeutics, 11099 North Torrey Pines Road, Suite 160, La Jolla, CA 92037, USA.